Improved Active Region Designs for Mode Locking in Quantum Cascade Lasers

M. Moradinasab*, M. Pourfath†*, and H. Kosina*

*Institute for Microelectronics, TU Wien, Gußhausstraße 27–29/E360, 1040 Wien, Austria

†Department of Electrical and Computer Engineering, University of Tehran, Tehran, Iran

e-mail: moradinasab@iue.tuwien.ac.at

1. Introduction

Quantum cascade lasers (QCLs) have progressed rapidly due to their intrinsic design potential [1]. These unipolar semiconductor lasers are based on intersubband transitions in multiple quantum-well structures. The design of alternating wells and barriers make QCLs a unique candidate to serve as a semiconductor source of ultra-short pulses in the mid-infrared region [2]. Ultrashort pulses which are generated in QCL media have been employed for various applications, such as non-linear frequency conversion, high-speed free space communication, and trace gas detection [3].

The most common technique for ultrashort pulse generation is mode locking which is realized either by an internal mechanism (passive mode locking) or by an external (active mode locking) [4]. In lasers with a relatively long gain recovery compared to the cavity round-trip time, the instability caused by a saturable absorber (SA) can often lead to passive mode locking [5]. It is demonstrated that fast gain recovery of QCLs exhibits two kinds of instabilities in the multi-mode regime: the Risken-Nummedal-Graham-Haken (RNGH)-like instability and one associated with spatial hole burning [6].

Advances in active-region designs and energy diagram optimization in the past few years have led to significant improvements of important characteristics of QCLs, such as their output power, emission bandwidth, characteristic temperature and efficiency [7].

In this work we investigate the active-region optimization and passive mode locking caused by a SA in a ring cavity QCL where only the RNGH instability is present.

2. Approach

Because of the large number of involved design parameters, performance improvement of QCLs requires a systematic multi-objective optimizer in conjunction with a simulation tool which has a good balance between computational speed and physical accuracy.

So far, optimization techniques proposed to design QCL structures are based on genetic algorithms [8–10]. Particle swarm optimization (PSO) [11] has been proposed as an alternative to traditional evolutionary algorithms. Unlike traditional evolutionary algorithms, particles in PSO do not perform the operation of genetic recombination between particles, but they work individually with social behavior in swarms. To study electronic transport in QCL, we employ a Pauli-master equation which is solved by the Monte-Carlo method [12]. Accurate results along with a relatively low computational cost render this approach as a good candidate for optimization studies.

In a QCL, the gain G is proportional to the population inversion Δn between the upper ($n = 3$) and lower ($n = 2$) laser states and can be written as [13]:

$$G = \sigma \Delta n = \sigma \frac{J}{q_0} \left[\tau_3 \eta_3 \left(1 - \frac{\tau_2}{\tau_{32}} \right) - \tau_2 \eta_2 \right], \tag{1}$$

where τ_2, τ_3 are the (total) lifetimes, τ_{32} is the intersubband lifetime between the states $n = 3$ and $n = 2$, and σ is the transition cross section. In the case of a QCL based on a superlattice active-region, Eq. (1) can still be applied with the $n = 3$ state being the lower state of the upper miniband and the $n = 2$ the upper state of the lowest miniband.

Instability mechanisms in QCLs are evaluated by linear stability analysis [6] in which the criteria for RNGH instability is expressed in terms of the parametric gain $g(\Omega)$ as a function of the resonance frequency Ω:

$$g(\Omega) = -\frac{c}{2n} \mathrm{Re} \left[l_0 \frac{(\Omega T_1 + i)\Omega T_2 - 2(p-1)}{(\Omega T_1 + i)(\Omega T_2 + i) - (p-1)} + \frac{\gamma \hbar^2 (p-1)}{\mu^2 T_1 T_2} \frac{(\Omega T_1 + i)(3\Omega T_2 + 2i) - 4(p-1)}{(\Omega T_1 + i)(\Omega T_2 + i) - (p-1)} \right], \tag{2}$$

where T_1 is the gain recovery time , T_2 is the dephasing time, l_0 is the linear cavity loss, μ is the matrix element of the lasing transition, γ is the SA coefficient, and p is the pumping above lasing threshold for

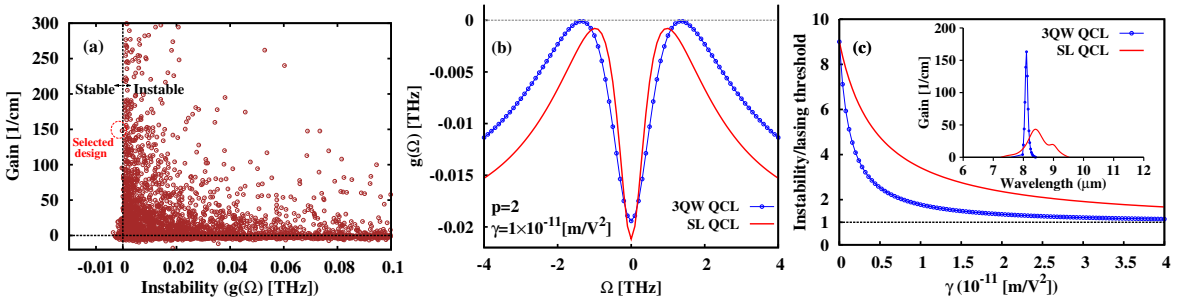

Fig. 1: (a) PSO results for a 3QW active-region QCL. (b) The parametric gain $g(\Omega)$ as a function of the resonance frequency Ω. (c) The pumping ratio p at which the RNGH instability sets in as a function of the SA coefficient. Inset: Optical gain spectra obtained for two optimized active-region QCLs.

$\gamma = 0$. Based on this analysis, each mode which is identified by the resonance frequency Ω is stable if the parametric gain is positive, otherwise it is unstable.

3. Results

We consider the laser gain as a figure of merit and define the instability criterion to satisfy stability conditions. At each iteration of the optimization process, for a set of geometrical parameters and the applied electric field, required instability parameters (T_1, T_2, and μ) are extracted and the parametric gain (Eq. 2) is evaluated. If the stability condition (Eq. 2) is not satisfied, a new set of parameters is selected for the next iteration. The well and barrier thicknesses and the applied electric field are modified until maximum gain and laser operation below the instability threshold are achieved.

Two different active-region designs are studied. The first one is the original design based on a three quantum well (3QW) active-region separated from the injection/relaxation region by a tunneling barrier [14] and the second one consists of a superlattice (SL) active-region [15].

Figure. 1(a) exhibits the optimization results for the 3QW active-region design. Based on developed optimization algorithm, many structures are generated and the one with the largest optical gain and satisfied instability condition is selected. The instability characteristics for the two optimized active-region QCLs are compared in Fig. 1(b). Because of the larger matrix element (μ) and longer upper laser state lifetime (τ_3), which is approximately equal to the gain recovery time (T_1), the SL active-region QCL indicates more stable operation and higher instability threshold (see Fig. 1(c)). However, the matrix element and lifetimes of the lasing transition, which are the key parameters in linear stability analysis, are proportional to optical gain (see Eq. 1). As we can see in the inset of Fig. 1(c), 3QW QCL exhibits larger optical gain at nearly the same wavelength. The optical gain of 3QW structure is maximized by delocalizing the lasing states which increases the lifetimes τ_3 and τ_2. Because of the bound states in SL active-region QCL, there is no significant lifetime variation, however, due to the larger matrix element, better instability condition is achieved.

4. References

[1] Y. Yao, A. J. Hoffman, and C. F. Gmachl, Nature Photonics **6**, 432 (2012).
[2] C. Y. Wang, L. Kuznetsova, V. M. Gkortsas, L. Diehl, F. X. Kärtner, M. A. Belkin, A. Belyanin, X. Li, D. Ham, H. Schneider, P. Grant, C. Y. Song, S. Haffouz, Z. R. Wasilewski, H. C. Liu, and F. Capasso, Opt. Express **17**, 12929 (2009).
[3] R. Paiella, F. Capasso, C. Gmachl, D. L. Sivco, J. N. Bailargeon, A. L. Hutchinson, A. Y. Cho, and H. C. Liu, Science **290**, 1739 (2001).
[4] V.-M. Gkortsas, C. Wang, L. Kuznetsova, L. Diehl, A. Gordon, C. Jirauschek, M. A. Belkin, A. Belyanin, F. Capasso, and F. X. Kärtner, Opt. Express **18**, 13616 (2010).
[5] H. A. Haus, IEEE J. Select. Topics Quantum Electron. **6**, 1173 (2000).
[6] A. Gordon, C. Y. Wang, L. Diehl, F. X. K. a, A. Belyanin, D. Bour, S. Corzine, G. Höfler, H. C. Liu, H. Schneider, T. Maier, M. Trocolli, J. Faist, and F. Capasso, Phys. Rev. A **77**, 053804 (2008).
[7] I. I. Zasavitskii, Quantum Electronics **42**, 863 (2012).
[8] A. Bismuto, R. Terazzi, B. Hinkov, M. Beck, and J. Faist, Appl. Phys. Lett. **101**, 021103 (2012).
[9] P. A. Sanchez-Serrano, D. Wong-Campos, S. Lopez-Aguayo, and J. C. Gutiérrez-Vega, Opt. Lett. **37**, 5040 (2012).
[10] D. Gagnon, J. Dumont, and L. J. Dubé, Opt. Lett. **38**, 2181 (2013).
[11] *Swarm Intelligence* (Morgan Kaufmann Publishers Inc., San Francisco, CA, USA, 2001).
[12] O. Baumgartner, Z. Stanojevic, and H. Kosina, in *Simulation of Semiconductor Processes and Devices (SISPAD)* (2011), pp. 91–94.
[13] J. Faist, M. Beck, T. Aellen, and E. Gini, Appl. Phys. Lett. **78**, 147 (2001).
[14] C. Gmachl, F. Capasso, D. L. Sivco, and A. Y. Cho, Rep. Prog. Phys. **64**, 1533 (2001).
[15] J. Faist, D. Hofstetter, M. Beck, T. Aellen, M. Rochat, and S. Blaser, Quantum Electronics, IEEE Journal of **38**, 533 (2002).